Field Testing of the Fremont Bridge

MICHAEL J. KOOB AND JOHN M. HANSON

In July 1979, field tests were conducted on the Fremont Bridge on the Willamette River in Oregon to obtain strain and temperature measurements that would provide information on in situ and service load stress conditions. The behavior of the bridge was more dependent on temperature than on traffic. On a hot day when the temperature reached 100° F, the temperature differential between the exposed top and shaded bottom flange plates was 50° F. The maximum daily stress range in the tie girders due to the temperature differential was about 10 ksi. Where local bending occurred in the web plates, the maximum daily stress range was about 20 ksi. Comparison of strain readings on two days of comparable temperature, with light and heavy traffic, indicated that the stress range due to traffic was about 1-2 ksi. Dynamic recordings of strain were made at 12 selected category E details during typical traffic conditions. The passage of heavy vehicles typically caused stress ranges up to 1000 psi. The largest measured stress range of about 3000 psi was associated with the passage of a heavy mobile crane. The frequency of these stress ranges was estimated to be about 50 percent of the average daily truck traffic of 5400 vehicles. The bridge was also subjected to a controlled loading of four heavy vehicles weighing a total of 177 100 lb. The maximum stress range occurring on an instrumented cross section near the junction of the arch rib and tie girder was 750 psi. The maximum stress range at any other instrumented location was 2150 psi.

A comprehensive postconstruction evaluation study of the Fremont Bridge on the Willamette River in Oregon (1) was conducted for the Oregon State Highway Division (OSHD). The purpose of this study was to assess the long-range performance of main load-carrying, nonredundant tensile members and components of the structure.

A field testing program was carried out in July 1979 as part of the study. This program was intended to provide information about the behavior of the bridge under combined traffic and environmental conditions.

During the 10-day field testing period, one day was cool and partly cloudy and several days were hot and clear. The hottest day occurred on July 16, when the ambient temperature reached 100°F. Throughout the testing period, readings were taken at intervals of one or two hours or more often if the recording station was manned and selected gages were being monitored. Dynamic recordings of strain were made during typical traffic conditions. The bridge was also subjected to a controlled loading of four heavy vehicles weighing 177 100 lb.

DESCRIPTION OF BRIDGE

The Fremont Bridge is a three-span, stiffened steel tied arch 2159 ft in length, as shown in Figure 1. In this structure, the arch is loaded in compression and the tie girder is loaded in tension to counteract the thrust of the arch as well as in flexure to resist the live-load bending moments. The main span is divided into 28 panels at 44 ft, 10 in, for a total length of 1255 ft, 4 in. Each side span is divided into 10 panels at 44 ft, 10 in, for a total length of 448 ft, 4 in. Junctions between panels are numbered from 0 through 48. A description of the bridge and its design is given by Hedefine and Silano (2).

A typical section through the bridge, in the region where the arch is above the roadway, is shown in Figure 2. The orthotropic steel upper deck, carrying four lanes of westbound traffic, acts integrally with the tie girders. The bottom deck, carrying four lanes of eastbound traffic, is a reinforced concrete slab supported on stringers and floor beams. In the middle 896 ft of the bridge, where the arch ribs are above the tie girders, the bottom deck is suspended by hangers from the tie girders. Outside of this region, the bottom deck is framed into compression struts extending between the arch ribs and the tie girders.

Representative details of the orthotropic deck and tie girders are shown in Figure 3. The top flange is A36 steel, and the bottom flange is A588. The webs are 0.5 in thick except at the junctions with the arch ribs and pier columns. Typically, the lower 6 ft is fabricated from a high-strength, low-alloy steel that meets the requirements of ASTM A441, and the upper part is fabricated from A36 steel. This hybrid design reflects the integral action of the orthotropic deck and tie girders, with the neutral axis about 6 ft below the top flange. Welded construction is used throughout the tie girders, except for high-strength bolted field splices.

The arch ribs are box shaped and have a constant width of 4 ft. The depth of the web plates is 3 ft, 10 in; hence, the overall depth of the arch ribs varies depending on the flange plates, which have a maximum thickness of 2.25 in. High-strength, quenched and tempered ASTM A514 steel is used for the arch ribs, which are welded except for bolted field splices.

At the four junctions of the girders and arch ribs located at panel points 14 and 34, the cross section of the arch rib is changed from a box shape to three A514 strap plates in a vertical plane, each 3 in thick and 3 ft, 10 in deep. These three straps are stiffened by a welded diaphragm at middepth. The straps extend through slots in the top and bottom flanges of the girder.

The center section of the bridge, between panel points 14 and 34, was fabricated off site, trans-

Figure 1. Elevation of Fremont Bridge.

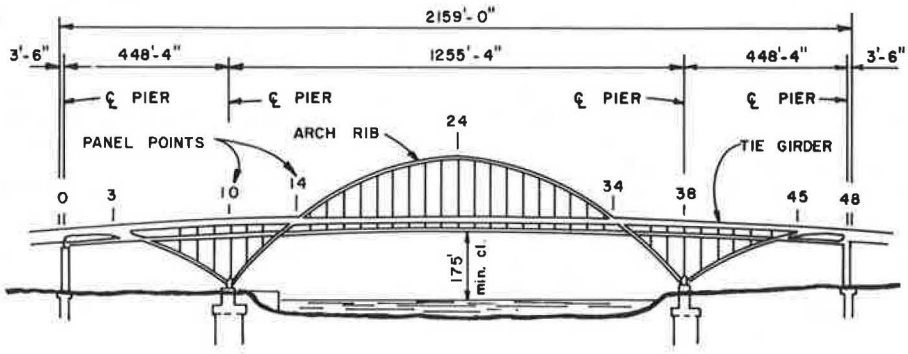

Figure 2. Typical section where arch is above roadway.

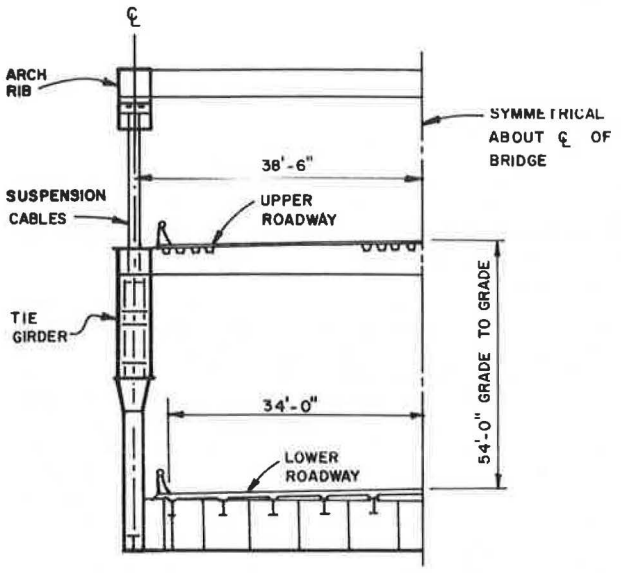

Figure 3. Representative details of deck and tie girder.

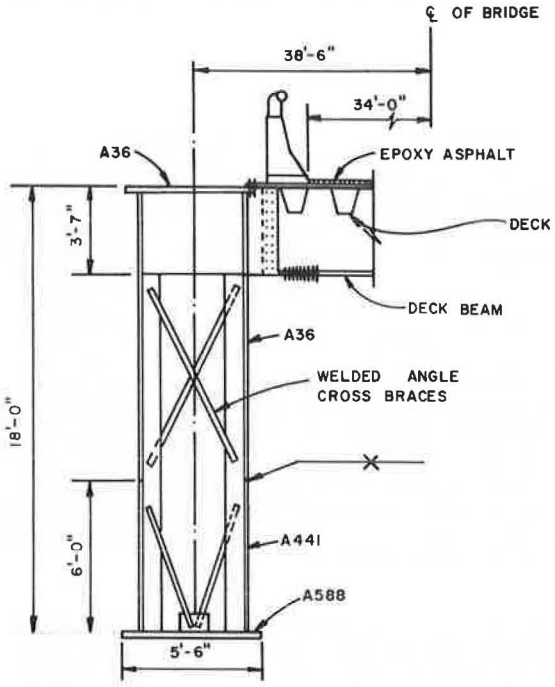

GIRDER SECTION

ported on barges, and erected by hydraulic jacking. A bolted splice connects the center and end sections, located within the junction of the tie girder arch rib. Heavy jacking stiffeners are also welded and bolted to the sides of the tie girder in this area.

The final coat of paint on the exterior of the bridge was a light shade of green.

INSTRUMENTED AREAS

It was decided that the best measure of the overall response of the bridge would be obtained by installing strain gages on four cross sections in the vicinity of panel point 14 in both the north and south tie girders. The locations of the instrumented sections, designated A, B, C, and D, are shown in Figure 4. Concern about the properties of a steel plate in the bottom flange near panel point 42 in the north tie girder led to installing instrumentation at a cross section in this region, designated section E.

Sections A, C, D, and E and section B were instrumented with six and sixteen 90° three-element strain gages, one element of which was parallel to the longitudinal axis of the member. At panel point 14 on the north tie girder, three 3-element strain gages, designated group F, were installed on the north web plate adjacent to the heavy fillet welds attaching the strap to the web.

In conjunction with the strain gage instrumentation, thermocouples were installed in both the north and south tie girders at section B.

Additional instrumentation was installed at locations of details where conditions were believed to be susceptible to fatigue crack growth or where special study of strain response was desired. These details included (a) ends of horizontal stiffeners, designated group G; (b) reinforcement around vent openings, group H; (c) openings for lower deck hangers in the bottom flange, group I; and (d) junctions of deck beams and web plates, group J, as shown in Figures 5-8. A total of 12 details were instrumented by using two-element gages. The gages were located close to the detail. Wiring diagrams for the gages are shown in Figure 9. During most of the testing period, the longitudinal and transverse elements of the three-element gages were wired together to provide a single, temperature-compensated reading. Some readings were also made with all three elements wired separately to determine principal strains. Stress was calculated from these readings by assuming a modulus of elasticity of 29 million psi and Poisson's ratio of 0.3. A correction, usually small, was made in the computed stresses to account for biaxial effects. The longitudinal and transverse elements of the two-element gages were wired together throughout the testing period.

To facilitate the strain measurements, a central recording station was established inside the north tie girder between panel points 14 and 15. Twisted, shielded, 18-gage, 3-conductor wires were used to connect the gages to the recording station.

MEASURED TEMPERATURES

Selected measurements on the tie girders are shown in Figure 10. Review of the data shows that the temperature distribution was uniform before sunrise (at 4:00 a.m.). At sunrise, or approximately 6:00 a.m., the south web and top flange of the south tie girder were exposed to the sun, if the day was clear, and would begin warming. Peak temperatures on both the south web and top flange were reached at about 1:00 p.m.

The north tie girder was shaded by the upper roadway until late afternoon. The peak temperature of the top flange was reached at about 1:00 p.m., whereas the peak temperature of the north web occurred in early evening, at about 6:00 to 8:00 p.m., after it was exposed to the sun.

The maximum temperature measured was 144°F, which occurred on the top flange of the south tie girder on July 16, 1979, when the ambient temperature was 90°F. Surfaces not exposed to the sun were always close to the ambient temperature. The maximum temperature differential between the top flange and side plates of both tie girders was about 50°F.

Figure 4. Location of instrumentation at panel point 14.

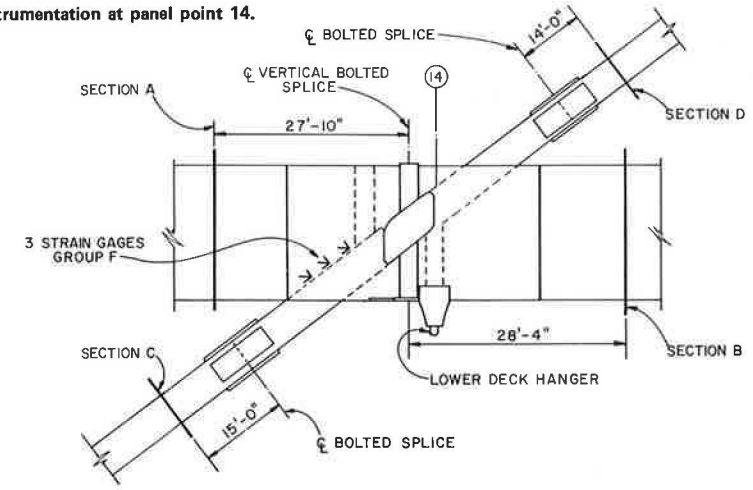

Figure 5. Group G gages at end of horizontal stiffener.

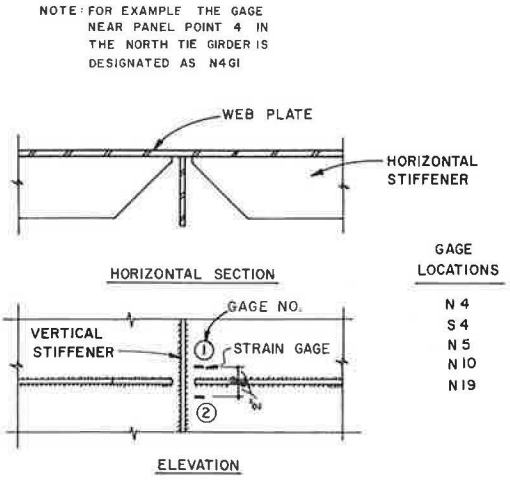

Figure 6. Group H gages at cover plates at vent opening.

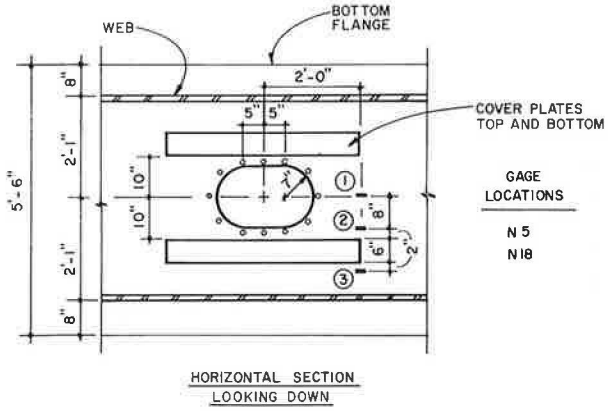

Figure 7. Group I gages at opening in bottom flange.

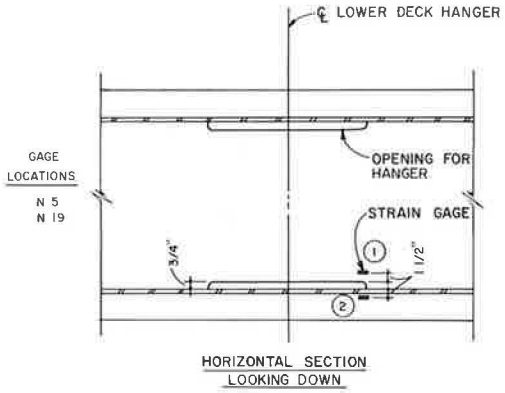

Figure 8. Group J gages at junction of deck beam and web of tie girder.

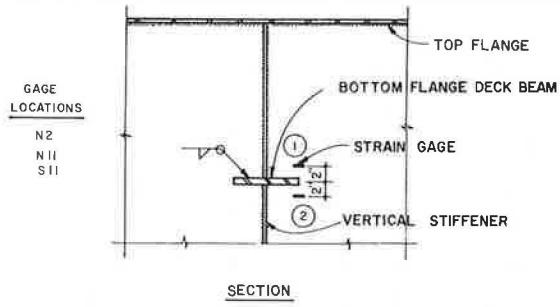

STRESSES UNDER TRAFFIC

Figures 11-15 show the change in stress at selected gage locations near panel point 14, computed from the measured strain during the period from July 12 through July 17. Data from a representative thermocouple are also presented in each figure.

Strain at gages SA1 and SA2 located on the top flange plate at section A in the south tie girder is shown in Figure 11. The temperature was obtained from thermocouple S1 located on the top flange plate at section B in the south tie girder. The abrupt change in temperature at approximately 1:00 p.m. is due to the passing of the shadow of the arch rib over section B. Maximum stress range is about 12 ksi. Note, however, that the shadow of the arch rib does not pass over the gages at section A.

Strain at gage SB2, located on the top flange plate at section B in the south tie girder, is shown in Figure 12. The temperature was obtained from thermocouple S1, which is adjacent to the strain gage. At this location, the strain responds in close relation to temperature. The maximum stress range is approximately 10 ksi.

Strain at gages NA2 and NA5, located on the top

and bottom flange plates, respectively, at section A in the north tie girder, is shown in Figure 13. Thermocouple N1 was located on the top flange plate at section B in the north tie girder. Stress ranges are about 11 and 4 ksi at these two locations.

In Figure 14, the strain at gages NB3 and NB13 is shown. These gages are located on the top and bottom flange, respectively, at section B in the north tie girder. Temperature measurements were obtained from thermocouple N1, which is located adjacent to gage NB3. Stress ranges of 8 and 5 ksi are apparent at the two locations.

Data from strain gages on the tie girder web plates indicate that out-of-plane bending occurs. Figure 15 shows this effect at section B on the

Figure 9. Strain gage wiring diagrams.

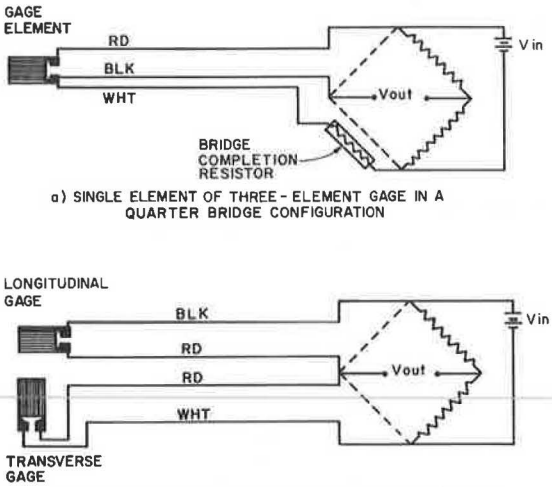

Figure 10. Measured temperatures.

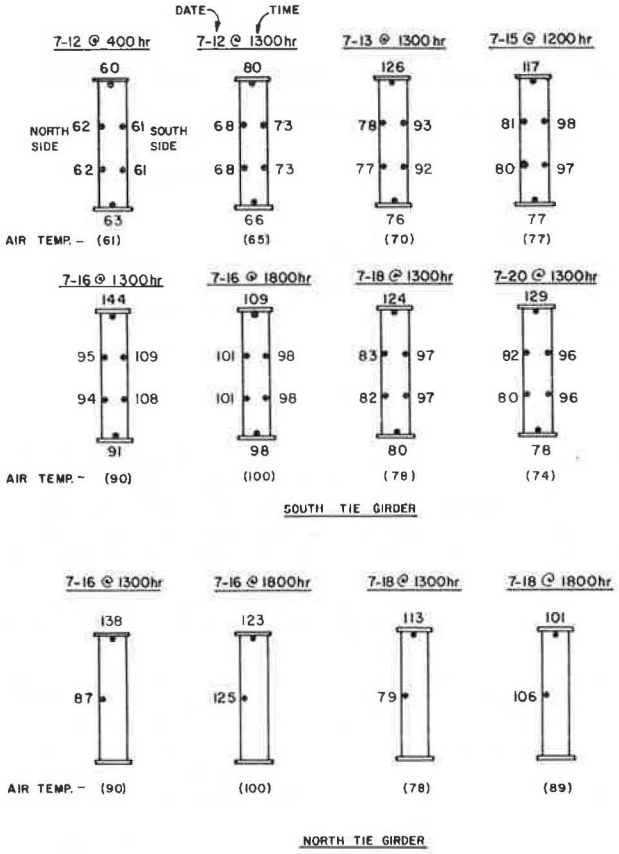

Figure 11. Strain gages SA1 and SA2 and thermocouple S1.

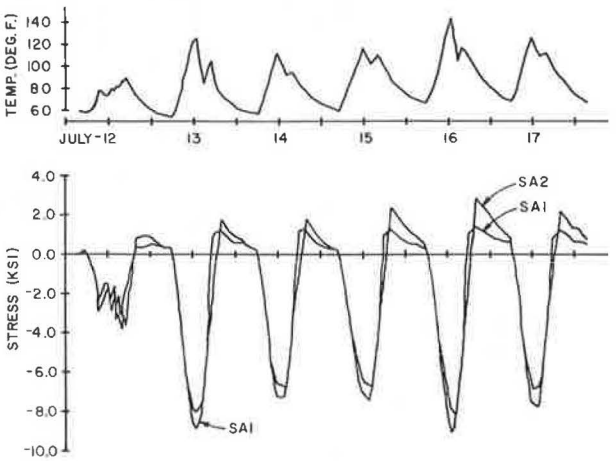

Figure 12. Strain gage SB2 and thermocouple S1.

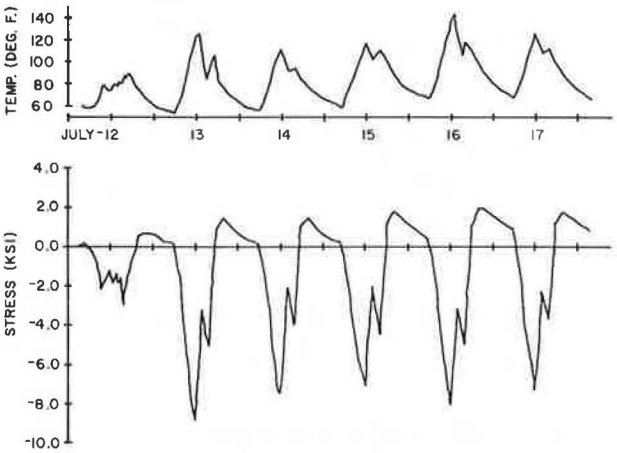

Figure 13. Strain gages NA2 and NA5 and thermocouple N1.

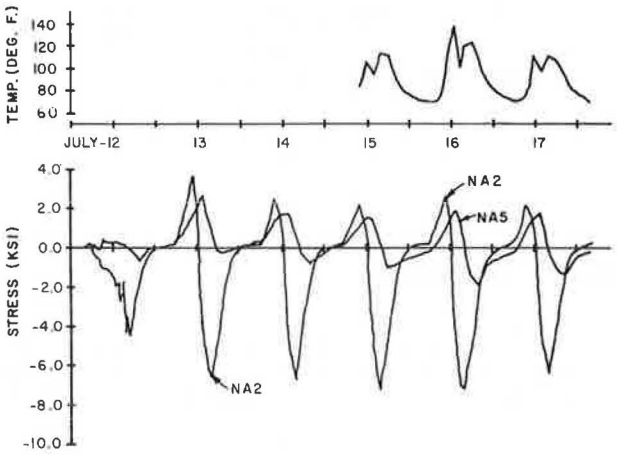

Figure 14. Strain gages NB3 and NB13 and thermocouple N1.

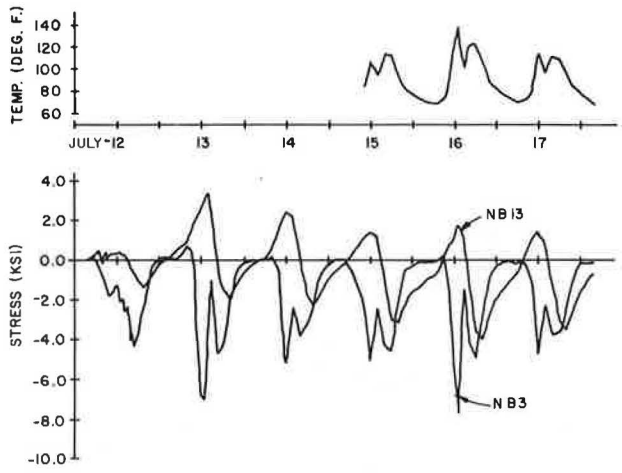

Figure 15. Strain gages NB9 and NB10 and thermocouple N2 and air.

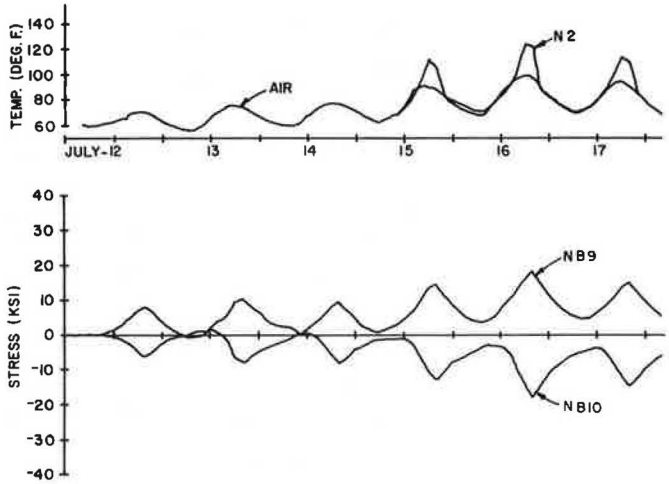

north web of the north tie girder. Longitudinal stresses computed from strains are plotted for gages NB9 and NB10, which are located on opposite sides of the web plate midway between stiffeners. Bowing of the plate apparently occurs daily. The maximum daily stress range is approximately 20 ksi, although the average stress is fairly uniform.

It is evident from these figures that the stress variations are repeatable and closely related to temperature. The heavy traffic periods in the morning and afternoon have little apparent effect.

Readings made on two days with similar temperatures but different traffic conditions were compared. These days were Sunday, July 15, when traffic was light, and Tuesday, July 17, when traffic was normal. The differences indicated that the stress range due to traffic was about 1-2 ksi.

STRESSES UNDER CONTROLLED LOADING

During the field testing, the bridge was subjected to a loading of four vehicles weighing a total of 177 100 lb. This test was conducted early in the morning on July 15 to minimize temperature effects. Both static and dynamic tests were conducted. Traffic was excluded from the bridge.

In the static loading test, the four trucks were positioned side by side in two rows on the upper deck in the two adjacent traffic lanes nearest to the north tie girder. Strain response was measured with the vehicles positioned at selected panel points along the bridge.

Figure 16. Measured strains at gages NB2 and NB4 under controlled loading.

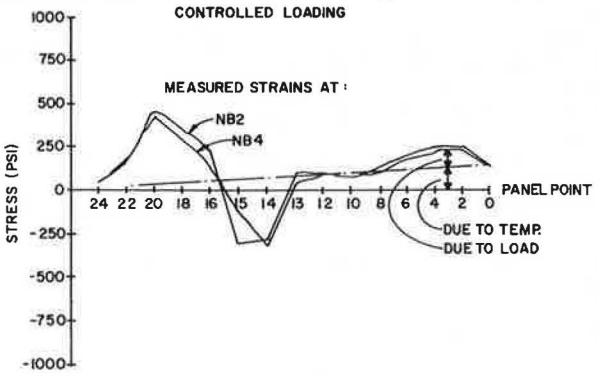

Figure 17. Strain gages NB13 and NB15.

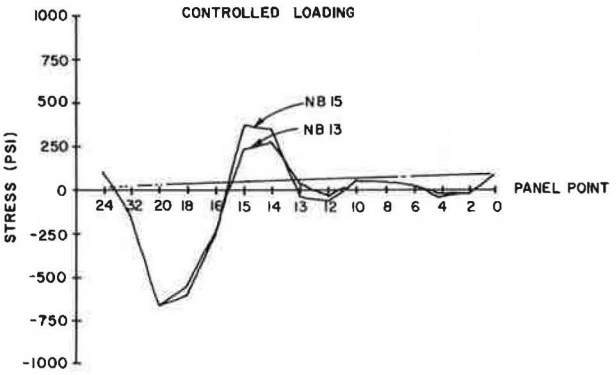

Figures 16 and 17 show computed stresses from strains measured at section B in the north tie girder. The ordinate and abscissa correspond to the longitudinal stress and the location of the vehicles, respectively. Note the departure of the ordinate from the base line at the conclusion of the test. This departure is attributed to the change in ambient temperature during the time period in which the test was conducted, between 6:00 and 7:30 a.m. The measured strains were quite small, corresponding to stresses less than 750 psi.

It may be noted that the strain response is greater when the vehicles are between panel points 14 and 24 than when they are positioned between panel points 14 and 0. This is apparently due to the varying stiffness of the structure. Between panel points 14 and 0 the tie girder is supported at each panel point by a vertical column, whereas between panel points 14 and 24 the tie girder is suspended by cables. When the vehicles were at panel point 10 (vertical column over pier), stress at all sections was essentially zero.

Data were also recorded in analog form by using a nine-channel strip chart recorder. Two groupings of gages were monitored; the first was on selected details, and the second was on gages from section B on the north tie girder.

Data were obtained during run A when the vehicles were parked at each panel point. In the dynamic test, run B, the four trucks were driven in a group across the bridge at approximately 15 mph in the same lanes used for the static tests. Data from gages recorded during the passage of vehicles in run

B are shown in Figure 18. The stress levels in both runs were quite low. The maximum static stress recorded in run A was 2150 psi at gage N19G2; the maximum dynamic stress in run B was 2100 psi at gage N19I2. The dynamic response followed the same general pattern as the static response.

To induce impact loads and provide information on impact factors, 2-in-thick boards were placed across the roadway at panel points 18.5 and 10.5. The output recorded during these runs indicated that the impact excited higher modes of vibration but there was only a slight magnifying effect on the strain readings.

STRESSES AT FATIGUE-SENSITIVE DETAILS

Dynamic recordings of strain under normal traffic were made at the fatigue-sensitive details from July 16 to July 20. The gages were divided into groups, and each was recorded for time periods of 1-4 h. Generally, significant strain response was associated with the passing of a truck. However, the representative stress "signatures" were very small. Typical data are shown in Figure 19. The maximum stress range, at gage N5I1, was 1250 psi. More typical values are 400-900 psi. As mentioned previously, the response for gages at the same detail was similar.

It is also of interest to compare these data with those obtained under the controlled loading shown in Figure 18. In all cases, the stress ranges recorded under the controlled loading were somewhat greater.

STRESS RANGES AND FREQUENCY OF OCCURRENCE

On July 17, dynamic strain recordings were made at four selected details for a period of approximately 2 h, between 10:30 a.m. and 2:30 p.m. From previous recordings, the strains at these details appeared to be larger than at other locations. Data obtained from the eight gages at these four details, during an interval of about 1 min, are shown in Figure 20.

A histogram of the stress computed from strain at one gage from each of the four details was developed from the dynamic recordings. The minimum strain that could be recognized on the recording corresponded to a stress of about 300 psi. In developing the histogram, each peak to valley or valley to peak on the recording in excess of 300 psi was therefore considered to be one-half of a stress cycle. On this basis, the number of stress cycles in 300-psi increments (ignoring cycles below 300 psi) was obtained and plotted in the histograms shown in Figure 21.

An effective Miner's stress range (S_{re}) was computed from the data in these histograms by using the following relation:

$$S_{re} = (\Sigma \gamma_i S^3_{ri})^{1/3} \quad (1)$$

Figure 19. Dynamic strain response under normal traffic.

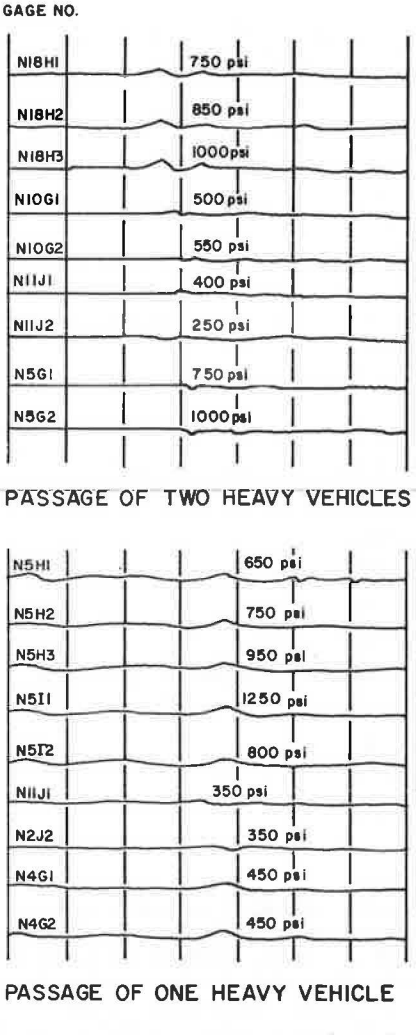

Figure 18. Data from run under moving truck loading.

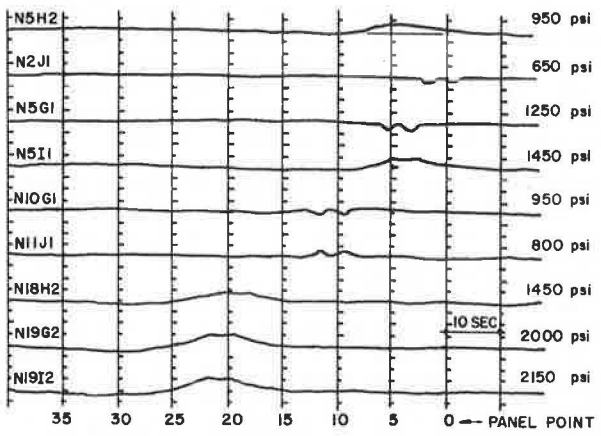

Figure 20. Dynamic strain response at four details on July 17, 1978.

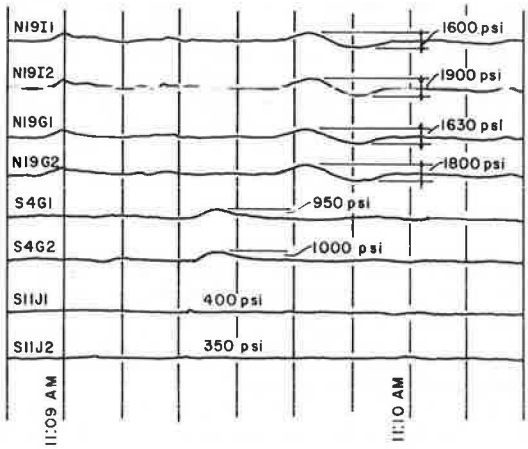

Figure 21. Histograms of stress cycles based on data obtained during 2-h period.

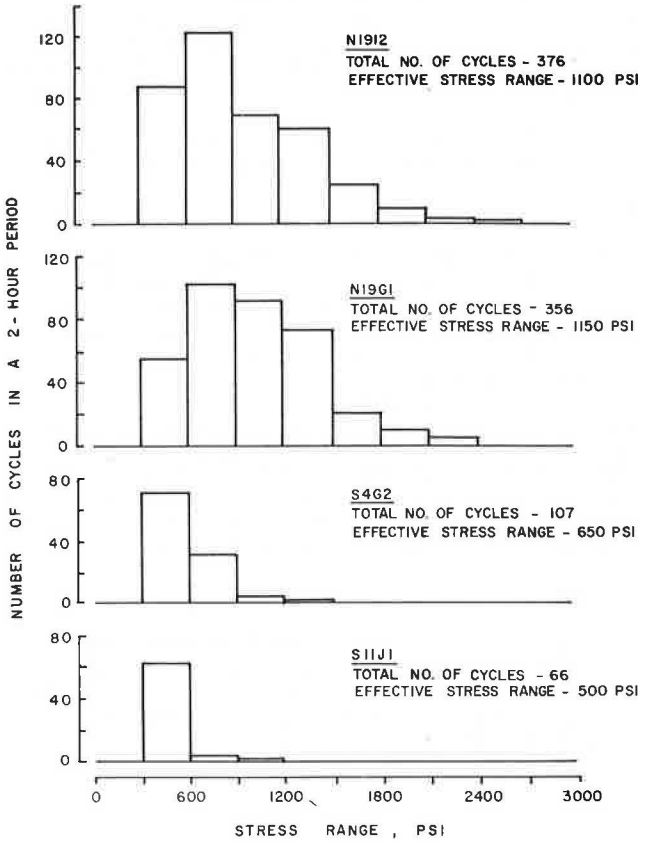

Figure 22. Dynamic strain response of gages during passing of mobile crane.

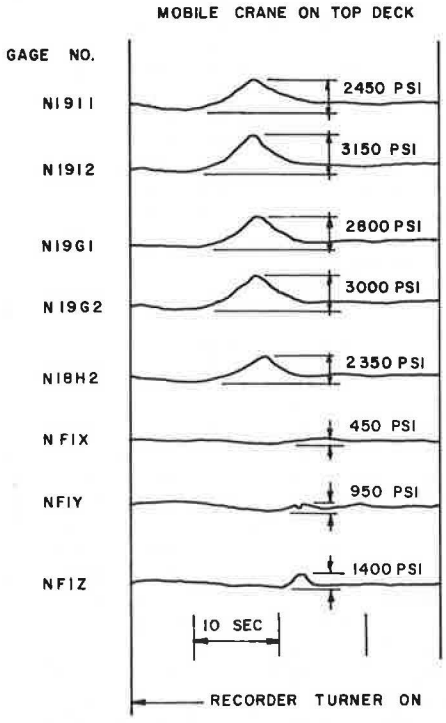

NOTE:
NFIX — ELEMENT PARALLEL TO ARCH RIB
NFIY — ELEMENT AT 45 DEGREES TO ARCH RIB
NFIZ — ELEMENT PERPENDICULAR TO ARCH RIB

where γ_i is the proportion of the total cycles falling within a particular interval i, corresponding to a stress range S_{ri}. The effective stress range for each histogram is shown in Figure 21. During this 2-h period, the maximum strain was observed at gage N19I2 and corresponded to a stress range of about 2550 psi. A total of 376 cycles were measured at this gage. The maximum effective stress range of 1150 psi was obtained at gage N19G1.

COMPARISON OF TRAFFIC WITH DYNAMIC RECORDINGS

Beginning at 2:40 p.m. on July 19, an effort was made to correlate dynamic strain recordings, or signatures, with observation of the traffic. This was found to be very difficult; only occasionally could a signature be associated with a specific vehicle such as a logging truck.

The vehicle that produced the largest recorded stress range was identified as a mobile crane on the top deck. The stress signatures from this load are shown in Figure 22. Except for the magnitude of the response, the signatures are similar to those of other heavy vehicles. It is interesting to compare the signatures for gages N19I2 and N19G2 with the signatures obtained during the controlled loading tests shown in Figure 18. The signatures are similar except that the two rows of vehicles passing in quick succession in the controlled loading test are distinguishable and the stress ranges are somewhat lower.

DISCUSSION OF RESULTS

The field testing indicated that three conditions induced stress variations in the tie girders. Most of the small-amplitude but high-cycle stress variation came from the passage of heavy vehicles. A small stress variation associated with the buildup of traffic was also observed. A large-amplitude stress variation occurred daily with temperature change.

The maximum measured stress range associated with the passage of a heavy vehicle was 3.15 ksi at a hanger slot in the bottom flange of the north tie girder near panel point 19. Most of the measured stress ranges at the instrumented details were less than 1 ksi, although stress ranges up to 2.5 ksi were measured near panel point 19. An effective Miner's stress range of 500-1150 psi was determined from data at each of four locations.

It was estimated that the number of cycles per day would be about eight times the number of cycles shown in Figure 21 for a 2-h period at midday. On this basis, the number of expected daily cycles at gages N19G and N19I is approximately 3000. The number of cycles at other locations is smaller.

Information supplied by OSHD indicated that the annual average daily traffic (ADT) on the bridge in 1978 was 58 775 vehicles. A projection to the year 2000 indicated that the ADT may be 93 400 vehicles. Approximately 9 percent of the vehicles crossing the bridge may be classified as trucks. Assuming that the ADT was 60 000 vehicles during the field testing, the average daily truck traffic (ADTT) should be about 5400 vehicles. Thus, the ADTT is about 1.8 times the rough estimate of 3000 cycles/day from the details near panel point 19. It should also be noted that the maximum stress range recorded at the details near panel point 19 under the controlled four-truck loading was 2.15 ksi, or approximately twice the maximum effective stress range under normal traffic.

The largest stress variations were related to the effects of temperature and particularly to direct exposure to the sun. As the sun passed over the bridge, the exposed surface of the south and then the north tie girder absorbed substantial heat. The maximum measured temperature was 144°F and occurred on the top flange of the south tie girder on July 16, 1979, when the ambient temperature was 90°F. Surfaces not exposed to the sun were always close to the ambient temperature. Temperature differentials of 50°F between the top and bottom flange plates and 20°F between the outside and inside web plates were measured in both tie girders.

The strain measurements indicated that the state of stress in the tie girders in the vicinity of the arch ribs is very complex. Maximum daily stress ranges in the longitudinal direction of the tie girders were about 10 ksi on the hot days. Where local bending occurred in the web plates, the maximum daily stress ranges were about 20 ksi.

Strain readings on two days of similar temperature conditions were compared in an effort to estimate the underlying stress variation due to light and heavy traffic. These days were Sunday, July 15, and Tuesday, July 17. Gages on section NB and strain gage NF1 were selected for the comparison. Readings were compared between 2:00 and 6:00 p.m. Most of the differences in stress are less than 1 ksi at section NB. Stress values obtained from gage NF1 show a change of 2 ksi in the web of the tie girder perpendicular to the arch rib. Therefore, the underlying stress variation due to traffic is believed to be about 1-2 ksi.

Because the density of the traffic may vary even during peak periods, it is thought that the underlying stress variation due to traffic should be considered to occur, at most, 50 times a day. This variation combines with the stress ranges associated with the passage of heavy vehicles.

CONCLUSIONS

Field testing indicated that stress ranges in the tie girders under traffic were generally less than 2 ksi and only infrequently 3 ksi. The number of cycles varied with the location, but it did not exceed the ADTT. However, the temperature of plates exposed to the sun may be as much as 50°F higher than the temperature of plates in the shade, which is always close to the ambient temperature. The nominal stress may change by about 10 ksi as a result of daily thermal effects. Where local bending was present, the daily stress range was about 20 ksi.

ACKNOWLEDGMENT

The field test discussed in this paper was part of a larger study conducted under the overview of a technical committee that included chairman Walter J. Hart and John C. Jenkins of OSHD and Carl Hartbower, Herbert A. Schell, and Frank Sears of the Federal Highway Administration.

Wiss, Janney, Elstner and Associates, Inc. (WJE), was assisted in the study by the following consultants and subcontractors: John W. Fisher of Lehigh University; Ammann and Whitney; Materials Research Laboratory, Inc.; and Testing Engineers, Inc. Other members of the WJE project staff included Boris Bresler, Robert Iding, and Daryl W. Boggs.

REFERENCES

1. J.M. Hanson, M.J. Koob, and B. Bresler. Post-Construction Evaluation Study, Fremont Bridge (Willamette River), I-405-Bridge 2529. Oregon State Highway Division, Salem, Dec. 30, 1981, 181 pp.
2. A. Hedefine and L.G. Silano. Design of the Fremont Bridge. ASCE National Structural Engineering Meeting, Portland, OR, Preprint 1210, April 1970.

Publication of this paper sponsored by Committee on Dynamics and Field Testing of Bridges.

Seismic Design of Curved Box Girders

C.P. HEINS AND I.C. LIN

The seismic response of single and continuous curved steel composite box girder bridges has been predicted by an equivalent structure load method. This method has been developed by computing equivalent structural stiffnesses of the entire bridge for the three displacement directions (x, y, z) and rotation. These stiffnesses are then used to evaluate corresponding natural frequencies (ω_x, ω_y, ω_z, and ω_t) by using a single degree of freedom system. The induced accelerations are then determined from the response spectrum curves. The results of these analyses are then used to develop a series of empirical equations for direct design.

As a result of the 1964 Alaskan earthquake, the 1971 San Fernando earthquake, and, more recently, the 1978 Santa Barbara earthquake (1), bridge structures in the United States have undergone considerable destructive forces. These earthquakes caused bridge professionals to reassess the design techniques that had been applied until that time for seismic design.

A prime force in such modifications has been the California Department of Transportation (Caltrans) and the California-based professional organization, Applied Technology Council (ATC). The present 1977 American Association of State Highway and Transportation Officials (AASHTO) bridge code (2), as related to seismic design, was greatly influenced by the work developed by Caltrans. This code suggests an equivalent static force method for simple structures and, when the structure is complex--as in curved bridges, for example--a computer-based response spectrum or dynamic analysis should be considered.

In the present 1977 AASHTO code, most engineers would use the seismic coefficient method (SCM) because computer-oriented dynamic programs may not be available or are not amenable for direct design. However, the SCM may give erroneous results when used for design under seismic conditions (3), as experienced by Caltrans. Caltrans in fact has used